Low-cost processing of pure and Al-doped capped ZnO nano powder for industry scale applications

P. N. Mishra[a], D. Pathak[a,b,*], P. K. Mishra[a], V. Kumar[c]
[a]*Department of Physics, Sri Sai University, Palampur, HP, India*
[b]*School of Physics and Materials Science, Shoolini University of Biotechnology & Management Sciences, Bajhol, Solan 173212, HP, India*
[c]*Department of Applied Science, CT institute of Technology and Management, Jalandhar, India*

Zinc oxide and metal-doped oxides are multifunctional nanomaterials used in the Nano World due to their distinctive characteristics and unique physical and chemical properties such as extraordinary chemical stability, anti-corrosion, low electrons conductivity, a broad range of radiation absorption, high photo stability, and tremendous heat resistance. To synthesize zinc oxide and Al-doped ZnO nanostructures with the inexpensive sol-gel method is our research objective, further we aimed to analyse the characterization of undoped and Al-doped ZnO nanopowder. Al-doped zinc oxide with compositional formula $Al_xZn_{1-x}O$ (x = 0, 2, 4, 6) was synthesized using Zinc acetate dihydrate (Zn $(CH_3COO)_2$. $2H_2O$) as a precursor, Sodium hydroxide (NaOH) and distilled water were used as a second-hand medium for the preparation of the solution. Ethanol (CH_2COOH) served as a versatile intermediate and was used as a solvent. The X-ray diffraction peaks suggest a hexagonal wurtzite crystal structure which matches with the pattern of the standard hexagonal structure of ZnO and Al-doped zinc oxide in all samples. X-ray diffraction result exhibits good crystallinity. The scanning electron microscopy images confirm the clear formation of spherical ZnO nanopowder and the change of the morphology of the nanopowder with the incorporation of the aluminium. The scanning electron microscopy results are in adjacent settlement with that estimated by the Debye-Sheerer formula created on the X-ray diffraction pattern. The usual crystallite size of Al-doped zinc oxide decreases by an increase in Al concentration with capping without varying the temperature. X-ray diffraction and scanning electron microscopy with energy dispersive x-ray analysis revealed that all samples crystallize in polycrystalline nature with wurtzite lattice. The result of energy dispersive x-ray analysis characterization shows that the ZnO nanopowders with no other main adulterated phase. Extant learning ventures this as a low-cost method for the synthesis of pure and capped Al-doped ZnO for industry scale applications.

(Received November 2, 2021; Accepted January 11, 2022)

Keywords: Zinc oxide (ZnO), Sol-gel method, Nanopowder, characterization, Al-doped zinc oxide (AZO), X-ray diffraction, Scanning electron microscopy, Energy dispersive x-ray analysis

1. Introduction

Metal oxide nanopowder cultivates a new category of imperative materials that are increasingly being used in research and technology-related applications. Currently, metal oxide nanomaterials are the utmost vastly produced nanomaterials. Their offered applications include catalysis, sensors, environmental remediation, medicine, varistors, solar cells, rubber, concrete, foods, cosmetics, and personal care products [1-11]. Subsequently, the inexpensive method to synthesise nanomaterial of the metal oxides such as copper oxide, titanium dioxide, magnesium oxide, and zinc oxide make them suitable than generally used costly nano silver oxide. Zinc Oxide nanomaterial is a great stimulating material due to its advantage in a diverse range of technological applications, low cost, non-toxicity, resource availability, and high physical and chemical stability

* Corresponding author: dineshpathak80@gmail.com
https://doi.org/10.15251/CL.2022.191.19

[12-14]. It is a wide band gap semiconductor, which has a direct band gap width of 3.37 eV [15]. The large energy band gap of the ZnO makes them transparent to visible light (400-700 nm). Besides, the wide band gap of ZnO has the least efficiency of photo catalytic activity of sunlight. To be an effective material, it is required to minimize the energy gap and increase the absorption of light. One of the tactics is doping. Doping is the intentional introduction of impurities in the material to amend its properties. The ZnO is one of the most extensive materials for numerous potential applications Al doping in ZnO increases the photo catalytic activity of the material due to this it is used as a laser diode, photodiode, Nano sensor, flexible and polymer-based solar cells, and an electrode in dye-sensitized solar cells. Zinc oxides of particle size in nanometre range have multi-functionality forms consideration in the research field correlated to its applications. Out of all it is in the interest of many research groups to work on the growth of ZnO and AZO centred on white light-emitting diode (LED) as a progressive source to provide bright and energy-saving light sources [16-18]. ZnO is an excessive electron transport layer in photovoltaic devices. It is cast-off in the arrangement of condensed or nanoparticle layers placed on top of a Fluorinated Tin Oxide cathode to enable electron extraction from the photovoltaic device. The good quality ZnO is due to its high n-type conductivity and proper energy levels. For the same reason, ZnO layers are used as electron carriers in quantum dot photo voltaic devices. Sol-gel and dip-coating methods produce pure and doped ZnO thin films, which are used as transparent conducting electrodes in photo voltaic [19]. The morphology can be changed by altering the solvent ratio of the solution [20, 21]. Transition (Fe, Co, Ni) metal-doped ZnO nanostructures are potential material for storage and transfer of data through electron spins along with electron charge as in conventional electronics and creating, manipulating or detecting light applications [22-24]. The extensive study of ZnO nanopowders doped with different ions such as Al, In, Ga, Co, Ni etc. has described improved photosensitive, and photo catalytic properties [25]. Amongst these, Al-doped ZnO (AZO) nanopowders have conductive and translucent properties in the visible region and hence can be used in transparent conductive oxide layer largely used in optoelectronic devices and photovoltaic [26]. The aluminium-doped ZnO (AZO) thin films are deposited on glass substrates with and without intrinsic ZnO (i-ZnO) bi-layer transparent conducting films and AZO acts as a transparent front-contact for thin-film solar cell. Analytically i- ZnO thin film behaves as an insulating layer, which stops the recombination of the photo-generated electron carriers and also decreases the lattice imperfections between CdS and AZO in CdS thin-film solar cell. In the arena of the solar cell, AZO thin film has been considered for its use as a window layer because of its low cost, and widespread disposal of its integral raw materials compared to Indium Tin Oxide (ITO). ZnO and AZO nanopowder exhibit distinct properties and have a various application like antibacterial property take in the manufacture of rubber and cigarette filters, antifungal and UV filtering used in calamine lotion, creams, ointments used to treat skin diseases and an additive in the production of concrete and ceramics and its anti-corrosive nature used as a coating agent in various paints.[27-40]ZnO and AZO Nano powders have been prepared by various physical and chemical methods such as thermal decomposition [41,42], spray pyrolysis [43,44], solvothermal reaction [45, 46], forced hydrolysis [47], reactive electron beam evaporation technique [48], sol-gel method [49,50], chemical vapour deposition [51], and hydrothermal method [52, 53]. They can also be manufactured into a vast range of morphologies [54] such as nanowires [55-59], nanorods [60, 61], nanocombs [62, 63], tetralegs [64], nanoflowers and nanosheet [65-67]. Amongst all these approaches Sol-Gel method is preferable because of low cost, lower production on scale temperatures, high-quality less agglomeration and short annealing times. Al-doped ZnO nanopowder was successfully synthesized by a simple sol-gel method specifically using polyvinyl alcohol (PVA) as a capping agent at a different concentration is capable of improving desired structural and optical properties. In this work, we have done a comparative study by XRD, SEM, and EDX of synthesised pure ZnO at different temperatures and Al-doped ZnO capped nanopowder for various Al concentrations with the same temperature. A low-cost method with possibility of industry scale up is presented.

2. Experimental detail

2.1. Materials and Method: Preparation of ZnO and AZO Nanopowder by Sol-gel Method

We carried out experimental work for obtaining ZnO nanopowder and AZO by the sol-gel method. The precursor Zinc acetate dihydrate (Zn $(CH_3COO)_2.2H_2O$) having a purity of 98%, ethanol (CH_2COOH) is used as a solvent and distilled water and Sodium hydroxide (NaOH) was

used as a medium in the synthesis of ZnO nanopowder. All the chemicals were provided by LOBA CHEMIE PVT.LTD. First, in a 100ml beaker 15 ml of distilled water is added with 2 gm Zinc Acetate, and separately in a 100ml beaker 15 ml of distilled water is added with 2 gm sodium hydroxide with continuous stirring for 5 minutes. In addition, about 2 ml of ethanol is drop-wise added with magnetic stirring to get a homogeneous solution. Ethanol takes care of the homogeneity and pH value of the solution and helps to make a stoichiometric solution to get Zinc oxide nanopowder. Keeping the stoichiometry in mind a 2gm batch of zinc oxide is prepared. Then the solution is left for 30 minutes which results in the formation of a white bulky precipitate of ZnO. The solution is then washed 8-10 times with distilled water and filter with the help of graded filter paper provided by WHATMANN to avoid adulteration of the sample. The residue obtained is put for drying in the oven at a temperature of about 200^{o}C for 4hrs. Finally, the aforementioned was set into an oxidizing furnace to execute heat treatment at 500 °C, 700 °C, and 750 °C. The yellowish-white zinc oxide nanomaterial in the form of powder was obtained. Fig 1 describes the steps followed during synthesis.

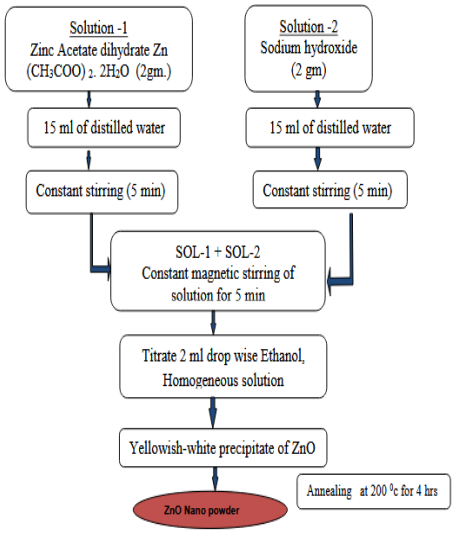

Fig. 1. Flow chart for synthesis ZnO nano powder.

The yellowish-white powder attained is exposed to calcination at some temperatures. First of all, a few obtained powders is put into the oven at a temperature of 500^{0} C for a few minutes. Similarly, for Powder X-ray diffraction patterns annealed under different temperature conditions. We prepared another sample by repeating the calcinations method for 700^{0}C and 750^{0}C. ZnO nanopowder was prepared through the sol-gel method ready for further characterization. To prepare Al-doped ZnO nanopowder firstly Aluminium nitrate nonahydrate (Al $(NO_3)_3$•$9H_2O$) was added into the Zinc Acetate dihydrate Zn $(CH_3COO)_2$ • $2H_2O$ to aid the aluminium source. The obtained solution was dissolved in a solution Mixed with 50 ml distilled water will gain concentration at 0% (AZO 0%), 2% (AZO 2%), 3% (AZO 3%) and 4% (AZO 4%) (g/ml), for the synthesis of Al_xZn_{1-x} O. All the chemical ingredients are A.R grade of HI-Media and were weighed in stoichiometric proportions for getting 5gms of final product and were dissolved in deionised water with constant Magnetic Stirring for 30 min. One of these sets left undoped, whereas, in the remaining set, Aluminium concentrations varied with x= 1 at. %, 2 at. %, 4 at. %, and 6 at. % Of Al in AlxZn1-xO, and were named hereafter as AZO 0%, AZO 2%, AZO 4%, and AZO 6% respectively. The metal nitrate solution was stirred uninterruptedly with the help of a magnetic stirrer. A homogeneous transparent solution is obtained. The 3:1 metal ion ratio solution with PVA was retained for all sets of samples. To obtain viscous solution metal nitrate was added drop by drop to the aqueous polyvinyl alcohol (PVA) capping agent at 500 ^{0}C and add10 ml NH_3 for gel formation. To get a homogeneous milk-white solution we implement Magnetic stirring continuously for 2-3 hrs. Then the gel was kept in an oven at 1500^{0} C to get a dried powder. Then samples were kept in a programmable muffle furnace, and the temperature was raised at the rate of 2 0 ^{0} C /min starting from room temperature up to 500 ^{0} C, then they were calcinations at this temperature for 1hr the flow chart of the samples preparation of AZO nano powder is shown in Fig. 2.

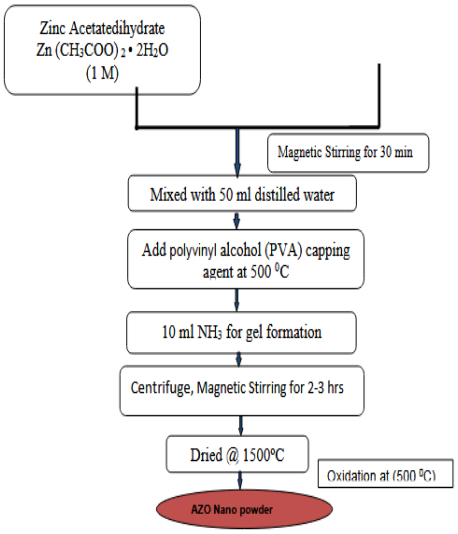

Fig 2. Flow chart for synthesis AZO nanopowder.

Al-doped ZnO is prepared 0% (AZO 0%), 2% (AZO 4%) and 6% (AZO 6%) subjected to calcinations at 500^0C temperatures then these samples are ready for structural characterisation.

2.3. Structural investigations

The prepared ZnO and Al-doped ZnO (AZO) were subjected to XRD studies using x-ray diffractometer make: Rigaku Corporation. The Powder X-ray diffractometer was performed on a 9 KW rotating anode x-ray generator with an NAI Scintillation counter detection system that is temperature dependent. The surface topography and composition studies were done by using a scanning electron microscope (SEM) to make JFEI Company Model: Nova Nano SEM-450 scans a focused electron beam over a surface to create a spitting image. The electrons emitted from the beam interact with atoms generally in the sample and results in which producing various signals that contain information about the surface topography and composition of the sample. SEM also can be coupled with EDX for elemental identification. The data generated by EDX analysis include spectra showing peaks analogous to the elements making up the true composition of the sample and then investigated. Image analysis and elemental recording of a set of samples are also possible. The learning of temperature effect on ZnO calcination treatments was done at 500 °C, 700 °C and 750 °C. In addition, to determine the effect of capped Al dopant on AZO in the same temperature be keen on structural characteristics and physical changed properties, we investigated both ZnO and AZO Nano powder comparatively.

3. Results and discussion

The synthesized powders were subjected to diffraction XRD imprint. Figure (3) demonstrate the X-ray diffraction outline for pure and capped samples with and without doping In the case of ZnO Nanopowder, from the diffraction pattern; we observed a graph which is plotted 2θ versus intensity. The sol-gel method has successfully resulted in ZnO crystalline structures. The samples planes are textured in direction (100), (101), (002), (102), (210), (103), (212) etc. This clearly shows the growth of the wurtzite structure as compared with the literature [68]. Capping and calcination temperature also appears to affect the crystallinity and grain size. The comparative plot explains that with increasing calcination temperature from 500^oC to 750^oC peak height rises as outcome diffraction peaks developed stronger and sharper, by this means indicates that the crystal quality has been improved and the size of particles grow bigger. This is alike for XRD studies shown that in the case of CuO nano powder by increasing temperature by the effect the full width at half maximum (FWHM) of peaks decreases indicating the improvement of the crystalline grain size [69].

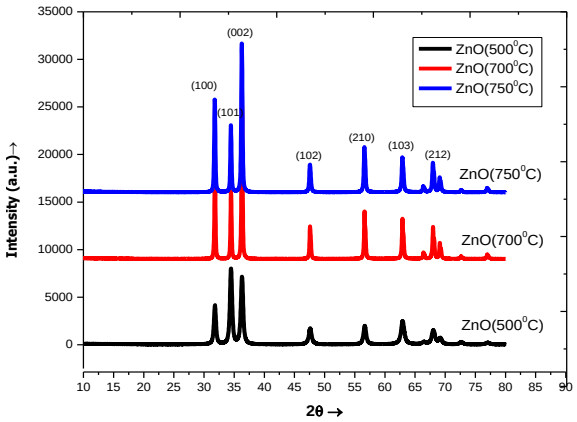

Fig. 3. XRD Pattern of ZnO Nano powder Synthesized at Calcinations Temperatures 500^{0}C, 700 ^{o}C and 750 ^{o}C.

The diffraction peaks at angles (2θ) of 31.36^o, 34.03^o,35.8 ^{o}, 47.16^o, 68.79^o, 69.45^o, 72.82^o and 77.33^{o}correspond to the reflection from (100), (101), (002), (102), (210), (103), (212) from Figure (3) it is comprehensive as of crystal planes that the nanopowder structure is composed of two interpenetrating hexagonal closed packed (hcp) sub lattices of the wurtzite ZnO structure. Debye-Sheerer formula is used to calculate the size. The mean size of the synthesised ZnO nanopowder is calculated and it has been valued using the full width at half maximum (FWHM). The equation is.

$$D = k \lambda / \beta \cos \theta \quad (1)$$

where k is the shape factor of the crystallite, which provides evidence about the curliness shape of the particle. Shape factor is given by

$$K= 4\pi. (Area) / (perimeter)^2 \quad (2)$$

The shape factor is 1 for spherical crystallites and less for other crystal. [70-71] Subject to the spherical morphology of the crystallites in ZnO nanopowder, the shape factor is calculated around k = 0.9 and used to determine the crystalline size. β is the average full width at half maximum intensity of the peak calculated for all samples, 'λ' is the wavelength of x-ray used in XRD and 'θ' is the Bragg diffraction angle. The mean size of as-prepared ZnO nanopowder was about 26 nm as calculated with Debye- Sheerer equation and shown in table 1. There are broadened peaks of ZnO, and this diffraction pattern and broadening were set up to a reliant on Miller indices of the equivalent sets of crystal planes. The diffraction line (0 0 2) in all samples are narrower than the line (1 0 1), and diffraction line (1 0 1) is narrower than the adjacent (1 0 0) line. This narrowness indicated in diffraction pattern an asymmetry in the crystallite shape. No peaks analogous to impurities were detected which confirm the purity of samples. By way of the increased temperature crystallinity of the particles, upsurges bring about particles to become bigger as per table (1). It is clear from (Fig.3) that the intensity of crystalline peaks rises with the increase in temperature signifying the improvement in the crystallinity of samples. Altogether, the peaks turn narrower as the temperature increases, presenting the increase in crystalline size and a decline in the full width at half maximum (FWHM), which point toward a possible change in the grain size of pure ZnO Thus, to develop small particles lower temperature is encouraging, as a higher temperature may diffuse grain boundaries pushing bigger crystals growth.

Table 1. Crystallite sizes of ZnO at various temperatures.

S. No.	**Growth Temperature (°C)**	FWHM	**Crystallite size (nm)**
1	500	0.68	14.19

2	700	0.34	28.50
3	750	0.31	34.17

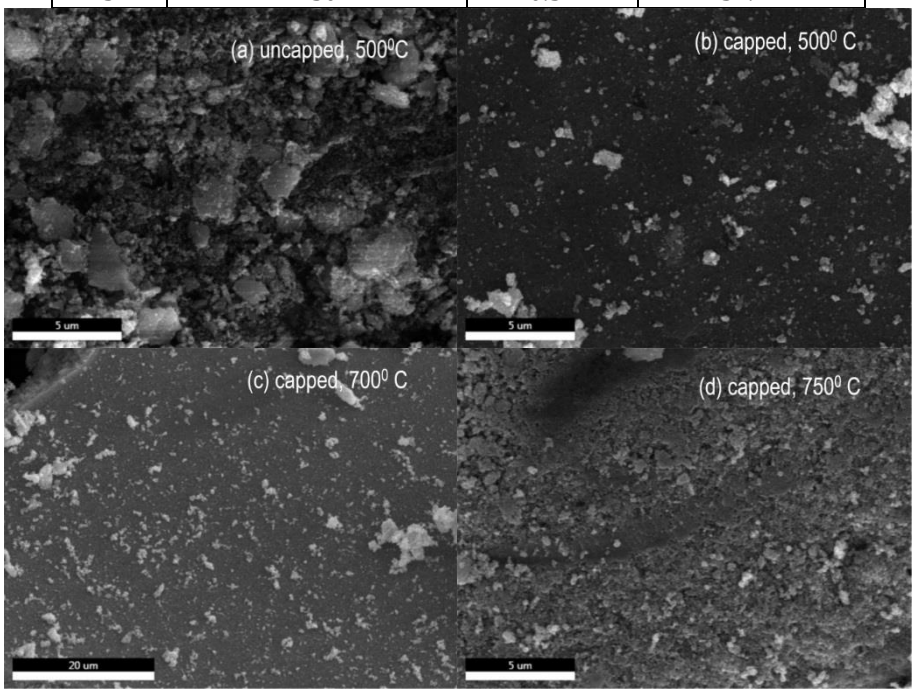

Fig. 4. SEM image of pure ZnO nanopowder with PVA and annealing (a) uncapped, 500^{0}C (b) capped, 500^0 C (c) capped, 700^0 C (d) capped, 750^0 C.

Scanning electron microscopy (SEM) magnifies the appearance of the sample morphological and structural studies. Fig. 4 displays the SEM morphology of the capped and uncapped ZnO nanoparticles at different calcination temperatures. SEM image approves the realisation of spherical grainy ZnO nanopowder and deviations in the morphology of the nanopowder with the increasing calcination temperature. XRD measurements showed that the particle size is between 14.19 nm and 34.17 nm which are supported by SEM analysis from the histogram. EDX study is an added add-on to the above results of samples.

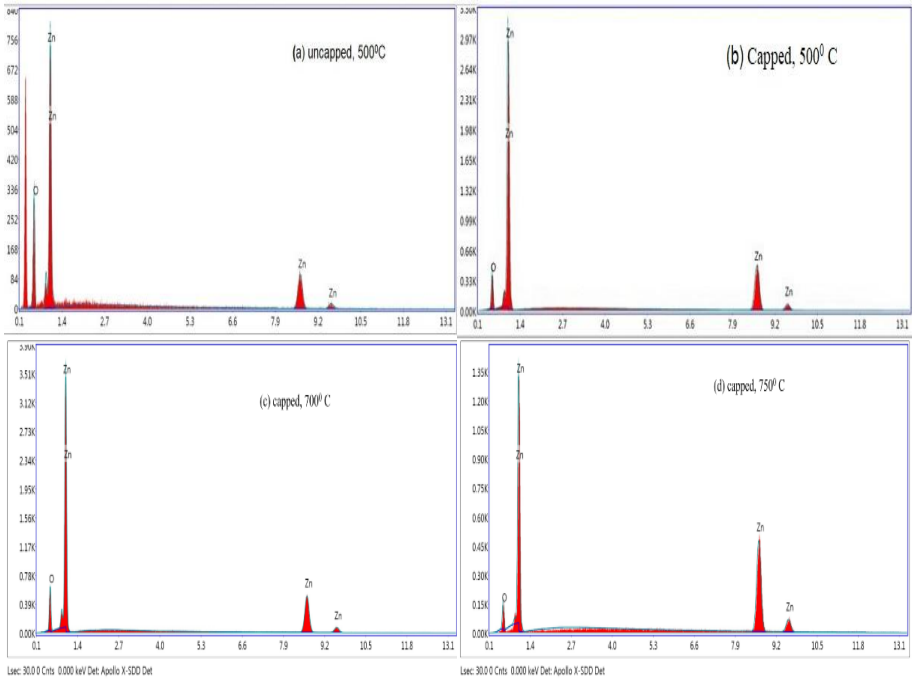

Fig. 5. EDX image of pure ZnO nanopowder with PVA and annealing (a) uncapped, 500^{0}C (b) capped, 500^0 C (c) capped, 700^{0}C (d) capped, 750^0 C.

An Energy Dispersive X-Ray Exploration (EDX) spectroscopy study was done to check the chemical composition of the prepared material. The presence of Zn and O was confirmed by the EDX study shown in Fig. 5, which displays the EDX spectra of pure ZnO nanopowder samples using PVA capping agent at an altered temperature, Table 2. EDX of Pure ZnO nanopowder various temperatures which approves the synthesis of pure ZnO. These results are consistent with the XRD data.

Table 2. EDX of Pure ZnO nanopowder various temperatures.

	ZnO Uncapped/ (500^{0}C)		ZnO capped / (500^{0}C)		ZnO capped / (700^{0}C)		ZnO capped /(750^{0}C)	
Element	Weight %	Atomic %	Weight %	Atomic %	Weight %	Atomic %	Weight %	Atomic %
Zn	56.18	23.89	78.80	47.63	75.34	42.78	91.14	71.57
O	43.82	76.11	21.20	52.37	24.66	57.22	8.86	28.43

3.1. Effect of Al doping on ZnO Nanopowder

The prepared AZO nano powder sample of crystal was characterized by XRD and physical structural studied by examining with the XRD data. The XRD peaks were perceived and by comparing the observed data with the reported standard values (JCPDS NO.03-0888) of the sample. The peaks at 2θ = 31.36^o, 34.03^o, 35.8 ^{o}, 47.16^o, 68.79^o, 69.45^o, 72.82^o and 77.33^o correspond to the reflection from (100), (101), (002), (102), (210), (103), (212) with reflection planes of ZnO hexagonal wurtzite structure respectively. The diffraction peak has no other secondary phase impurity of oxides of Al or metallic Al. It shows that Al is amalgamated successfully into the ZnO lattice sites. It is definite from the diffraction pattern which is plotted 2θ versus intensity, the sol-gel method has successfully resulted in AZO crystalline structures. Figure (6) gives the XRD Pattern of Al-doped ZnO (AZO) nanopowder (a) 0% (b) 2% (c) 3% (d) 4% concentration The samples planes are oriented in direction (100) ,(101) ,(002) ,(102) ,(210) ,(103) ,(212) etc. which clearly shows the growth of wurtzite like structure as analogous with the literature[71].This preparation method of pure and doped ZnO powder by a low-cost sol-gel route has potential for industrial scale-up encouraging the applicability of this technique for cosmetics and other photo catalytic usages.

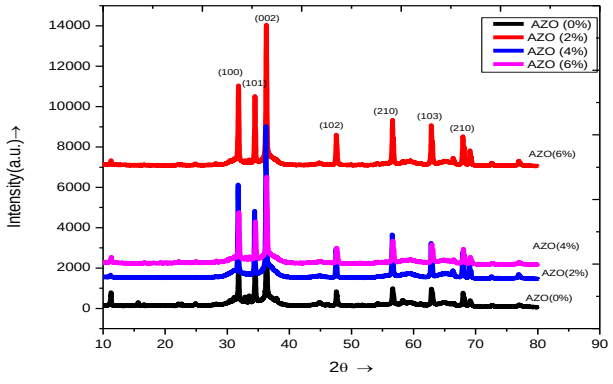

Fig. 6. XRD Pattern of Al doped ZnO (AZO) Nanopowder (a) 0% (b) 2% (c) 3% (d) 4%.

Table 3. Crystallite size of AZO particles at different concentration.

S.NO	Temperature ^{o}C	Al content (%) AZO Nano powder	Crystallite size (nm)
1	500 ^{0}C	0% (Uncapped)	35.05
2	500 ^{0}C	2%(capped)	24.03

3	500 ^{0} C	3%(capped)	24.57
4	500 ^{0} C	4%(capped)	18.89

The crystalline size of samples was calculated using Debye Scherer's formula using FWHM as enumerated in table 3 that is 35.05 nm, 24.03 nm, 24.57 nm, 18.89 nm for undoped AZO at 0%, AZO at 2%, AZO at 4%, AZO at 6%, respectively. The reduction in the crystallite sizes with growing Al concentrations in AZO with capping at the same temperature i.e. 500^0C can be analysed as the crystal growth gets reduced down with increasing Al concentrations. There is no second phase is perceived shown in the XRD results which revealed the hexagonal wurtzite structure of ZnO without any secondary phase. ZnO doped and capped doped XRD measurements showed that the particle size is between 35 nm and 18 nm which is supported by SEM analyses/EDX. As from the SEM images, it was observed that utmost of the sample particles were spherical, and the particles were well uniform in shape. A histogram for the SEM image was used to obtain the average grain size of the sample that is looking fit in accord with XRD results. Furthermost with growing in a concentration of Al and capping at a fixed temperature it seemed that agglomeration increases. Pure Al-doped zinc oxide (AZO 0%) displays that particle morphology is broken, asymmetrical, and round shape was observed. AZO particles with the increase of the dopant concentration of 2% and capping have resulted the large sizes and flat surfaces. The merger of Al^{3+} ions into Zn^{2+} lattice brings about the decrease of the crystalline nature of AZO as obtained [72]. The same results has also been observed in the dopant concentration of 4% and 6%. Finally with increase in the concentration of the Al-dopant capping without alteration in temperature has formed the different shapes of morphologies. The Al metal doping and PVA capping of AZO affected the crystallinity and crystal size along with morphologies [73-74].

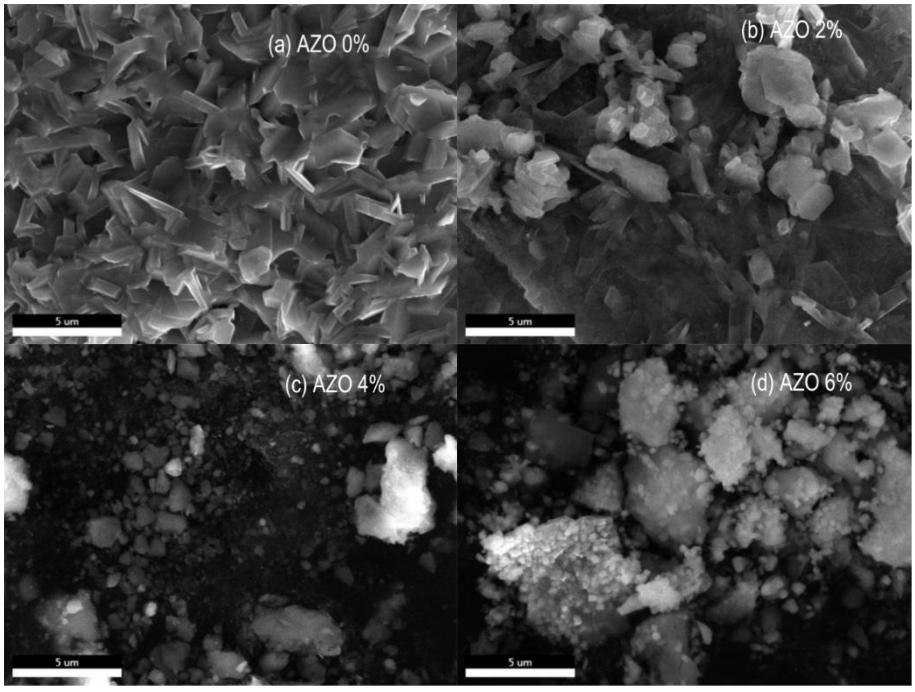

Fig. 7. SEM images of Al doped ZnO (a) AZO 0% (b) AZO 2% (c) AZO4% (d) AZO6%.

Using energy dispersive x-ray analysis (EDX) chemical composition of the prepared samples was analysed as shown in Fig. 8. EDX graphs of pure AZO nanopowder (a) AZO 0% (b) AZO 2% (c) AZO 4% (d) AZO6% displays that mass percentage (%) of Zn in Al doped capped AZO declines with increase Al doping concentration. The same was listed in Table 4.

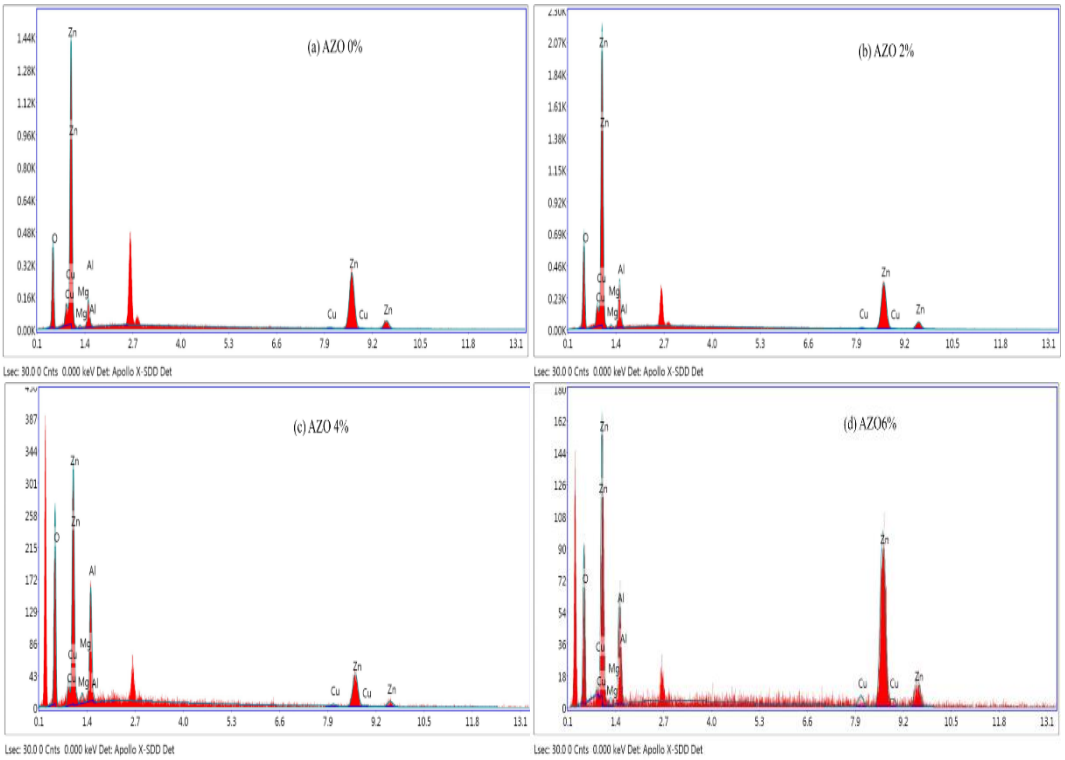

Fig. 8. EDX image of pure AZO nano powder (a) AZO 0% (b) AZO 2% (c) AZO 4% (d) AZO6%.

Table 4. EDX analysis result of Al doped ZnO (AZO).

Composite	AZO 0 %		AZO 2 %		AZO 4%		AZO6%	
Element	Weight %	Atomic %	Weight %	Atomic %	Weight %	Atomic %	Weight %	Atomic %
Zn	64.02	32.98	55.99	26.58	33.20	12.50	68.33	40.23
O	26.31	55.38	29.33	56.89	42.83	65.92	17.09	41.11
Al	7.70	9.61	12.53	14.42	19.75	18.02	10.49	14.96

Al-doped ZnO contains elements of C, O, and Mg (negligibly small %) element as evidently realized in figure 8 in synthesized nano powder due to unidentified reason and annealing temperature appears to affect the crystallinity of Al-doped ZnO nanopowder [75-76]. Also change of Al content and capping at same temperature did not considerably affect the phase structure and crystallite size of these systems. Finally we propose here this method as suitable for low cost industry scale purpose to miniaturize structures of metal oxides to nano level.

4. Conclusion

In this study, the ZnO at different temperatures and capped AZO at the same temperature at different concentrations were successfully synthesized through an inexpensive sol-gel synthesis method. The structural properties of ZnO and AZO nanopowders were studied using the X-ray diffraction technique (XRD) and crystalline size was calculated. The XRD outcome definite the proficiency of the synthesis process, evidencing the production of crystalline ZnO nanopowder with hexagonal wurtzite structure. The synthesized ZnO and capped Al-doped AZO powders are also characterized using Scanning Electron Microscope (SEM) which explains the morphology of the nanopowder that changes to the spherical shape and nanopowders were less agglomerate. EDX results confirmed the presence of zinc and oxygen in the synthesized pure ZnO nanopowders along with Al in AZO. It is clear that with the increasing temperature of ZnO samples calcination at 500^{o}C, 700^{o}C and 750^{o}C gives high-intensity fine peaks. With the increasing temperature from 500^{o}C to 750^{o}C crystallinity of the ZnO nanoparticles increases that is with size 14.19 nm to 34.17nm triggering particles to become larger. Thus, to get smaller particles lower temperature is favourable and making ZnO nanopowder suitable for cosmetics, and then industrial scale-up. It is observed that doping of aluminium at a different concentration (0%, 2%, 4%, and 6%) and capping at a certain temperature (500^{o}C) significantly reduces the crystallite size of AZO nanopowder i.e. 35.05nm, 24.03nm, 24.57nm, 18.89nm respectively. The disproportion of Al content and capping without changing temperature did not significantly stimulate the phase structure, but there is a decrease in the crystalline sizes of AZO with increasing Al concentrations. SEM images of the samples show the agglomeration increases with increasing PVA capped Al concentration. We observed that the size of samples can be controlled by increasing the temperature of ZnO Nanopowder and capping agent PVA with Al doping with different concentrations at the same temperature. Hence, low-cost sol-gel processing with the above parameters can thus be a striking method for the industrial production of pure and AZO Nano powders for various applications like in optoelectronics and UV sunscreen cosmetic industry.

Acknowledgements

Pooja Nag Mishra performed the experiments, and Dinesh Pathak mentored this research work. Pankaj Kumar Mishra and Vaneet Kumar has written the manuscript with analysis, performed experiment and collected data for Synthesis and Structural Characterization of Pure and Al –Doped Capped ZnO Nano Powder.

References

[1] C.S.S.R. Kumar, Nanotechnologies for the Life Sciences, 2006; https://doi.org/10.1002/9783527610419

[2] C. Klingshirn, Chemphys. 8(6), 782 (2007); https://doi.org/10.1002/cphc.200700002

[3] H. R. Safaei, M. R. Safaei, V. Rahmanian, Open Electro-chem. J. 4, 1 (2012).

[4] M. I. Baraton, Open Nanosci. J. 5, 64 (2011); https://doi.org/10.2174/1874140101105010064

[5] A. V. Budanov , Yu. N. Vlasov, G. I. Kotov , Yu. Y. Synorov , S. Yu. Pankov , E. V. Rudnev, V. E. Ternovaya , S. A. Ivkov, Chalcogenide Letters, 17 (9),457,(2020)

[6] M. A. Al-Mossawi, A. H. Al-Khursan, R. A. Al-Ansari, Recent Patents on Elect. Eng. 2, 226 (2009); https://doi.org/10.2174/1874476110902030226

[7] S. Singh, D. Kaur, D. Pathak, R. K. Bedi, Digest J. Nanometre. Biostruc 6(2), 689 (2011).

[8] M. D. J. Ooi, A. A. Aziz, M. J. Abdullah, N. H. Al-Hardan, Digest J. nanometres. Biostruc. 7(3), 1179 (2012).

[9] T. Goto, S. Yin, T. Sato, T. Tanaka, Int. J. Nanotech. 10(1-2), 48 (2013); https://doi.org/10.1504/IJNT.2013.050880

[10] D. Gingasu, I. Mindru, L. Patron, D. C. Culita, J. M. Calderon-Morero, L. Diamandescu, M.

Feder, O. Oprea, J. Phys. Chem. Solids 74(9), 1295 (2013); https://doi.org/10.1016/j.jpcs.2013.04.007
[11] I. Lacatusu, E. Mitrae, N. Badea, R. Stan, O. Oprea, A. Meghea, J. Funct. Foods 5(3), 1260 (2013); https://doi.org/10.1016/j.jff.2013.04.010
[12] T. J. Minami, J. Vac, Sci Techno. 17, 1765 (1999); https://doi.org/10.1116/1.581888
[13] C. K. N. Peh, L. Ke, G. W. Ho, Mater Lett. 64, 1372 (2010); https://doi.org/10.1016/j.matlet.2010.03.022
[14] Y. Zong, Y. Cao, D. Jia, S. Bao, Y. Lu, Mater Lett 64, 243 (2010); https://doi.org/10.1016/j.matlet.2009.09.032
[15] A. Mahroug, S. Boudjadar, S. Hamrit, L. Guerbous, Mater. Lett., 134 (2014); https://doi.org/10.1016/j.matlet.2014.07.099
[16] Z. L. Wang, J. Phys.: Condens. Matter 16, R829 (2004); https://doi.org/10.1088/0953-8984/16/25/R01
[17] J. L. Gomez, O. Tigli, J. Mater. Sci. 48, 612 (2013); https://doi.org/10.1007/s10853-012-6938-5
[18] L. Schmidt-Mende, J. L. MacManus-Driscoll, Mater.Today 10, 40 (2007); https://doi.org/10.1016/S1369-7021(07)70078-0
[19] R. Garcia Gutierrez, M. Barboza Flores, Advanced in Materials science in Engineering Journal, 5 (2012).
[20] Arun S. Menon, Nandakumar, Sabu Thomas, Indian Journal of Nanoscience 1(1), 16 (2013).
[21] J. Pearton, D. P. Norton, M. P. Evil, A. F. Hebard, W. M. Chen, I. A. Buyanova, J. M. Zavada, MRS Proc. 999, K03 (2007); https://doi.org/10.1557/PROC-0999-K03-04
[19] A. B. Djurišić, Y. H. Leung, Optical Properties of ZnO Nanostructures 2, 944 (2006). https://doi.org/10.1002/smll.200600134
[22] M. Silambarasan, S. Saravanan. T. Soga, e-J. Surf. Sci. Nanotech. 12, 283 (2014); https://doi.org/10.1380/ejssnt.2014.283
[23] H. Serier, M. Gaudon, M. Menetrier, Solid State Sci. 11, 1192 (2009); https://doi.org/10.1016/j.solidstatesciences.2009.03.007
[24] A. Verma, F. Khan, D. Kar, B. C. Chakravarty, S. N. Singh, M. Husain, Thin Solid Films 518, 2649 (2010); https://doi.org/10.1016/j.tsf.2009.08.010
[25] T. Ogi, D. Hidayat, F. Iskandar, A. Purwanto, K. Okuyama, Adv Powder Technol. 20, 203 (2009); https://doi.org/10.1016/j.apt.2008.09.002
[26] Y. Yang, X. Li, J. Chen, H. Chen, X. Bao, Hem. Phys.Letters 373(1-2), 22 (2003); https://doi.org/10.1016/S0009-2614(03)00562-1
[27] A. M. Schimpf, S. T. Ochsenbeina, R. Buonsanti, D. J. Milliron, D. R. Gamelin, Hem. Commun. 48, 9352 (2014); https://doi.org/10.1039/c2cc34635d
[28] R. Buonsanti, A. Llordes, S. Aloni, B. A. Helms, D. J. Milliron, Nano Lett. 11, 4706 (2011); https://doi.org/10.1021/nl203030f
[29] E. D. Gaspera, A. S. R. Chesman, J. van Embden, J. J. Jasieniak, ACS Nano 8, 9154 (2014); https://doi.org/10.1021/nn5027593
[30] X. Liang, Y. Ren, S. Bai, N. Zhang, X. Dai, X. Wang, H. He, C. Jin, Z. Ye, Qi Chen, L. Chen, J. Wang, Yizheng Jin, Chem. Mater. 26, 5169 (2014); https://doi.org/10.1021/cm502812c
[31] G. Garcia, R. Buonsanti, E. L. Runnerstrom, R. J. Mendelsberg, A. Llordes, A. Anders, T. J. Richardson, D. J. Milliron, Nano Lett. 11, 4415 (2011); https://doi.org/10.1021/nl202597n
[32] S. D. Lounis, E. L. Runnerstrom, A. Bergerud, D. Nordlund, D. J. Milliron, Am. Chem. Soc. 136, 7110 (2014); https://doi.org/10.1021/ja502541z
[33] A. M. Schimpf, S. D. Lounis, E. L. Runnerstrom, D. J. Milliron, D. R. Gamelin, J. Am. Chem. Soc. 137, 518 (2015); https://doi.org/10.1021/ja5116953
[34] U. Zum Felde, M. Haase, H. Weller, J. Phys. Chem. B 104, 9388 (2000); https://doi.org/10.1021/jp0010031
[35] J. M. Xu, L. Li, S. Wang, H. L. Ding, Y. X. Zhang, G. H. Li, Cryst Eng. Comm. 15, 3296

(2013); https://doi.org/10.1039/c3ce40241j
[36] B. T. Diroll, T. R. Gordon, E. A. Gaulding, D. R. Klein, T. Paik, H. J. Yun, E. D. Goodwin, D. Damodhar, C. R. Kagan, C. B. Murray, Chem. Mater. 26, 4579 (2014); https://doi.org/10.1021/cm5018823
[37] L. De Trizio, R. A. Buonsanti, A. M. Schimpf, A. Llordes, D. R. Gamelin, R. Simonutti, D. J. Milliron, Chem. Mater. 25, 3383 (2013); https://doi.org/10.1021/cm402396c
[38] A. Agrawal, I. Kriegel, D. J. Milliron, J. Phys. Chem. C 119, 6227 (2015); https://doi.org/10.1021/acs.jpcc.5b01648
[39] B. Tandon, G. Shiva Shanker, A. Nag, J. Phys. Chem. Lett. 5, 2306 (2014); https://doi.org/10.1021/jz500949g
[40] S. Ghosh, M. Saha, V. D. Ashok, B. Dalal, S. K. De, J. Phys Chem. C 119, 1180 (2015); https://doi.org/10.1021/jp5107873
[41] O. Oprea, O. R. Vasile, G. Voicu, E. Andronescu, Digest J. Nanometre. Biostruc. 8(2), 747 (2013).
[42] O. R. Vasile, E. Andronescu, C. Ghitulica, B. S. Vasile, O. Oprea, E. Vaile, R. Trusca, J. Nano powder Res. 14(12), 1 (2012); https://doi.org/10.1007/s11051-012-1269-7
[43] L. C. Chen, C. H. Tien, Open Crystal. J. 2, 11 (2009); https://doi.org/10.2174/1874846500902010011
[44] P. Tonto, O. Mekasuwandumrong, S. Phatanasri, V. Pavarajarn, P. Praserthdam, Ceramics Int. 34(1), 57 (2008); https://doi.org/10.1016/j.ceramint.2006.08.003
[45] L. Kong, J. X. Yang, H. P. Zhou, Y. P. Tian, J. Y. Wu, B. K. Jin, BCurrent Nanosci. 5(4), 474 (2009); https://doi.org/10.2174/157341309789378113
[46] R. Al Asmar, J. P. Atanas, M. Ajika, Y. Zaatar, G. Ferblantier, J. L. Sauvajol, J. Jabbour, S. Juillaget, A. Foucaran, J. Crystal. Growth 279(3-4), 394 (2005); https://doi.org/10.1016/j.jcrysgro.2005.02.035
[47] O. Oprea, O. R. Vasile, G. Voicu, L. Craciun, E. Andronescu, Digest J. Nanometre. Biostruc. 7(4), 1757 (2012).
[48] N. Singh, Open Renew. Energy J. 5, 15 (2012); https://doi.org/10.2174/1876387101205010015
[49] J. J. Wu, S. C. Liu, Adv. Mater. 14(3), 215 (2002); https://doi.org/10.1002/1521-4095(20020205)14:3<215::AID-ADMA215>3.0.CO;2-J
[50] S. Baruah, J. Dutta, Sci. Tech. Adv. Mater., 2009, 10(1), 1-18.10 Current Organic Chemistry, 2014, 18, No. 2 Opera et al.
[51] G. Voicu, O. Oprea, B. S. Vasile, E. Andronescu, Digest J. Nanometre. Biostruc. 8(2), 667 (2013).
[52] R. Wahab, S. G. Ansari, Y. S. Kim, M. A. Dar, H. S. Shin, J. Alloys Compounds 461(1-2), 66 (2008); https://doi.org/10.1016/j.jallcom.2007.07.029
[53] H. He, Q. Yang, J. Wang, Z. Ye, Mater. Letters 65(9), 1351 (2011); https://doi.org/10.1016/j.matlet.2011.01.080
[54] C. P. Liu, R. C. Wang, C. L. Kuo, Y. H. Liang, W. Y. Chen, Recent Pat. Nanotech. 1(1), 11 (2007); https://doi.org/10.2174/187221007779814772
[55] Q. Li, V. Kumar, Y. Li, H. Zhang, T. J. Marks, R. P. H. Chang, Chem. Mater 17, 1001 (2005); https://doi.org/10.1021/cm048144q
[56] J. Zhang, L. Sun, H. Pan, C. Liao, C. Yan, New J. Chem 26, 33 (2002); https://doi.org/10.1039/b108172a
[57] M.-K. Li, D.-Z. Wang, Y.-W. Ding, X.-Y. Guo, S. Ding, H. Jinn, Mater. Sci. Eng. A 417, 452 (2007); https://doi.org/10.1016/j.msea.2006.10.089
[58] F. Fang, D. X. Zhao, J. Y. Zhang, D. Z. Shen, Y. M. Lu, X. W. Fan, B. H. Li, X. H. Wang, Mater. Lett 62, 1092 (2008); https://doi.org/10.1016/j.matlet.2007.07.073
[59] Q. Zhang, Y. Zhang, K. Yu, Z. Zhu, Vacuum 82, 30 (2008); https://doi.org/10.1016/j.vacuum.2006.12.016

[60] N. Huang, M. W. Zhu, L. J. Gao, J. Gang, C. Sun, X. A. Jiang, Appl. Surface Sci. 257(14), 6026 (2011); https://doi.org/10.1016/j.apsusc.2011.01.112

[61] P. Sangpour, M. Roozbehi, O. Akhavan, A. Z. Mosh Fegh, Current Nano sci. 5(4), 479 (2009); https://doi.org/10.2174/157341309789377998

[62] G. Z. Jia, Y. F. Wang, J. H. Yao, Digest J. Nanometre. Biostruc. 7(1), 261 (2012).

[63] D. H. Fan, R. Zhang, Y. Li, Solid State Commun. 150(39-40), 1911 (2010); https://doi.org/10.1016/j.ssc.2010.07.036

[64] J. Singh, P. Kumar, D. K. Late, T. Singh, M. A. More, D. S. Joag, S. Tiwari, K. S. Hui, K. N. Hui, O. N. Srivastava, Digest J. Nanometre. Biostruc. 7(2), 795 (2012).

[65] A. J. Hashim, M. S. Jaafar, A. J. Ghazali, N. M. Ahmed, Digest J. Nanometre. Biostruc. 7(2), 487 (2012).

[66] H. H. Kou, X. Zhang, Y. L. Du, W. Ye, S. X. Lin, C. M. Wang, Appl. Surface Sci. 257(10), 4643 (2011); https://doi.org/10.1016/j.apsusc.2010.12.108

[67] Agnieszka Kołodziejczak-Radzimska, Teofil Jesionowski, Materials, 2833 (2014); https://doi.org/10.3390/ma7042833

[68] B. I. Kharisov, Recent Pat. Nanotech. 2(3), 190 (2008); https://doi.org/10.2174/187221008786369651

[69] K. SowriBabu, A. Ramachandra Reddy, Ch. Sujatha, K. Venugopal Reddy, Mater Lett. 99, 97 (2013); https://doi.org/10.1016/j.matlet.2013.02.079

[70] Jaber Attou, Boujemaâ, Hamid. Ez-Zahraouy, Mediterranean Journal of Chemistry 7(5), 308 (2018); https://doi.org/10.13171/mjc751911261230la

[71] D. Pathak, R. K. Bedi, D. Kaur, Optoelectron. Adv. Mat. 4(5), 657 (2010).

[72] W. H. Zhang, W. D. Zhang, J. F. Zhou, J. Mater. Sci. 45, 209 (2010); https://doi.org/10.1007/s10853-009-3920-y

[73] M. Chitraa, K. Uthayarania, N. Rajasekaranb, E. K. Girijac, Physics Procedia 49, 177 (2013); https://doi.org/10.1016/j.phpro.2013.10.024

[74] B. Ayadi, L. El Mir, S. Alaya, K. Djessas, Nanotechnology 18, 445072 (2007); https://doi.org/10.1088/0957-4484/18/44/445702

[75] Q. Hou, F. Meng, Sun, J. Nanoscale Research Letters 8, 144 (2013); https://doi.org/10.1186/1556-276X-8-144

[76] H. Munawaroh, S. Wahyuningsih, A. H. Ramelan, Materials Science and Engineering 176, 12049 (2017); https://doi.org/10.1088/1757-899X/176/1/012049